$MgFe_2O_4$ Magnetic Catalyst for Photocatalytic Degradation of Congo Red Dye in Aqueous Solution Under Visible Light Irradiation

Fahma Riyanti[1,2], Nurhidayah[1], Widia Purwaningrum[1,2], Nova Yuliasari[1], and Poedji Loekitowati Hariani[1,2*]

[1]*Department of Chemistry, Faculty of Mathematics and Natural Sciences, Universitas Sriwijaya, Jalan Palembang-Prabumulih, Indralaya, Ogan Ilir 30662, Indonesia*

[2]*Research Group on Magnetic Materials, Department of Chemistry, Faculty of Mathematics and Natural Sciences, Jalan Palembang-Prabumulih, Indralaya, Ogan Ilir 30662, Indonesia*

ARTICLE INFO

Received: 3 Jan 2023
Received in revised: 13 May 2023
Accepted: 15 May 2023
Published online: 23 Jun 2023
DOI: 10.32526/ennrj/21/20230002

Keywords:
$MgFe_2O_4$/ Photocatalytic degradation/ Visible light irradiation/ Congo red

*** Corresponding author:**
E-mail:
puji_lukitowati@mipa.unsri.ac.id

ABSTRACT

In this study, $MgFe_2O_4$ was successfully synthesized through the coprecipitation method using the precursors $Fe(NO_3)_3 \cdot 9H_2O$ and $Mg(NO_3)_2 \cdot 6H_2O$. The $MgFe_2O_4$ product was characterized using XRD, SEM-EDS, VSM, UV-DRS, and FTIR. The catalyst was used for the photocatalytic degradation of Congo red dye under visible light irradiation. The variables of the photocatalytic degradation included solution pH, Congo red concentration, H_2O_2 concentration, and irradiation time. The $MgFe_2O_4$ synthesized has magnetic properties, with a saturation magnetization value of 17.78 emu/g and a band gap of 1.88 eV. A degradation efficiency of 99.62% was achieved under specific conditions, including a Congo red concentration of 10 mg/L, a solution pH of 6, an H_2O_2 concentration of 2.5 mM, and an irradiation time of 180 min. The degradation efficiency without H_2O_2 was observed to be 83.45%. The photocatalytic degradation of Congo red followed the pseudo-first-order kinetics model with a rate constant (k) of 0.0167 min^{-1} and a half-life ($t_{1/2}$) of 41.49 min. The total organic carbon (TOC) removal of 84.58% indicated that the mineralization of Congo red had occurred. The effectiveness of photocatalytic degradation decreased from 99.62% to 94.50% (<5%) after five cycles of photocatalytic degradation. The results demonstrated that $MgFe_2O_4$ has a high Congo red dye degradation efficiency, can be regenerated, and is readily separated from the solution using a permanent magnet.

1. INTRODUCTION

Dyes are widely produced by industries of, among others, textiles, pharmaceuticals, soap, plastics, cosmetics, paper, and food (Wang et al., 2012; Ali et al., 2020). Azo dyes are the most widely used by industry, reaching 35% (Argote-Fuentes et al., 2021). They contain aromatic and N=N groups (Mezohegyi et al., 2012). The dyes have high toxicity and can even bioaccumulate in the food chain (Robinson et al., 2001; El Gaini et al., 2009). One of the azo dyes that is often used is Congo red. The dye has a structure that is resistant to oxidation and is difficult to degrade naturally, enabling it to survive in the environment for quite a long time (Sharma et al., 2021; Harja et al., 2022). Congo red has an aromatic structure that causes it to be carcinogenic and mutagenic (Saha and Mukhopadhyay, 2020). For this reason, an effective method for treating industrial wastewater containing dyes is necessary.

Various methods, such as adsorption (Harja et al., 2022), coagulation-flocculation (Habiba et al., 2017), ion exchange (Gao et al., 2021), photo-degradation (Jha and Chakraborty, 2020), electro-chemical oxidation (Sathiskumar et al., 2019), and direct membrane (Khumalo et al., 2019) have been used to reduce dyes. Some of the methods used have limitations. The dyes only undergo physical transformation without structural change, resulting in secondary pollutants that must be treated using other methods (Lum et al., 2020).

Advanced Oxidation Processes (AOPs) refer to methods that are inexpensive, effective, and capable of

Citation: Riyanti F, Nurhidayah, Purwaningrum W, Yuliasari N, Hariani PL. $MgFe_2O_4$ magnetic catalyst for photocatalytic degradation of Congo red dye in aqueous solution under visible light irradiation. Environ. Nat. Resour. J. 2023;21(4):322-332. (https://doi.org/10.32526/ennrj/21/20230002)

converting organic contaminants into smaller, harmless molecules (Jarariya, 2022). These methods use destructive techniques based on oxidation-reduction reactions with the help of photon energy. When a catalyst gains photon energy, electrons are excited from the valence band (VB) to the conduction band (CB) and leave the photo-generated hole (h^+). Furthermore, electron pairs/holes allow oxidation and reduction processes to occur on the surface of the photocatalyst (Valenzuela et al., 2002; Augugliaro et al., 2012) which can also be used for photocatalytic degradation processes repeatedly.

The effectiveness of degradation depends on the catalyst type and the irradiation source used (Oliveira et al., 2020). Semiconductor materials with wide band gaps (>3.0 eV), such as SnO_2, ZnO, and TiO_2, are corrosion-resistant but technically less effective at absorbing light in the UV region; only about 5% (Boudiaf et al., 2021). They are also unsuitable for the solar spectrum because it contains UV light and visible light irradiation of only 4.0% and 45%, respectively (Shahid et al., 2013). Thus, developing a photocatalyst capable of absorbing light in the visible region for practical applications is necessary.

Spinel ferrites have the general chemical formula AB_2O_4 where A is a metal ion, such as Co, Cu, Zn, Mg, Ni, Fe, Cd, or another metal, while B is iron(III) oxide (Fe_2O_3). These materials have narrow band gaps, thus effectively absorbing light in the visible region (Shahid et al., 2013). One of the ferrite compounds is $MgFe_2O_4$, which is an n-type semiconductor with a band gap between 1.7-2.4 eV (McDonald and Barlett, 2021). $MgFe_2O_4$ is a soft magnet with chemical and thermal stability (Shahjuee et al., 2019; Jarariya, 2022). The magnetic properties of ferrite compounds are advantageous in photocatalytic degradation processes because the photocatalyst can be removed from the solution quickly using a permanent magnet.

Combining a photocatalyst of ferrite compounds with H_2O_2 can increase degradation performance (Hariani et al., 2021). For example, the effectiveness of the photocatalytic degradation of $CoFe_2O_4$ with H_2O_2 on rhodamine B dyes was greater than that of $CoFe_2O_4$ under visible light irradiation (Nguyen et al., 2019). Likewise, the photocatalytic degradation of naphthalene using Fe_3O_4+H_2O_2 had greater effectiveness than without H_2O_2 (Zhang et al., 2019). H_2O_2 is an oxidant that can increase the number of hydroxyl radicals, thereby increasing the degradation efficiency. In addition, it is safe and does not threaten the environment because it decomposes into water and oxygen easily.

In this research, $MgFe_2O_4$ was synthesized using the coprecipitation method and applied to reduce the concentration of Congo red from solution. Several photocatalytic degradation variables, namely pH, initial concentration of dye, irradiation time, and H_2O_2 concentration, were investigated. An analysis of total organic carbon was carried out to prove the occurrence of dye mineralization. The photocatalyst was used repeatedly for the photocatalytic degradation of dyes to investigate their effectiveness and stability.

2. METHODOLOGY

2.1 Materials

Iron(III) nitrate nonahydrate $Fe(NO_3)_3{\cdot}9H_2O$, magnesium(II) nitrate hexahydrate ($Mg(NO_3)_2{\cdot}6H_2O$), ethanol (C_2O_6O), sodium hydroxide (NaOH), hydrochloride acid (HCl solution 37%), and Congo red dye ($C_{32}H_{22}N_6Na_2O_6S_2$) were obtained from Merck, Germany.

2.2 $MgFe_2O_4$ preparation

As much as 8.08 g $Fe(NO_3)_3{\cdot}9H_2O$ and 2.56 g $Mg(NO_3)_2{\cdot}6H_2O$ were dissolved in 120 mL of distilled water. Under nitrogen gas flow, a 1 M NaOH solution was dripped into the solution and stirred using a magnetic stirrer until the pH reached ±10. The precipitate was filtered, washed repeatedly with distilled water until pH 7, then dried in an oven at 100°C for 4 h and calcined at 500°C for 3 h to produce $MgFe_2O_4$ powder.

2.3 Characterization of $MgFe_2O_4$

The crystal structure and phase of the $MgFe_2O_4$ were characterized using X-Ray Diffraction (XRD PANalytical), CuKα radiation was performed at a wavelength (λ=0.15418 nm) and an accelerated voltage of 30 kV in the range of 2θ=10-90°. The functional groups before and after the photocatalytic degradation were characterized by Fourier Transform Infra-Red (FTIR Prestige 21 Shimadzu), obtained using the KBr pellet technique and scanning from 4,000-400 cm^{-1}. The elemental morphology and composition were characterized using a Scanning Electron Microscope-Energy Dispersive Spectrometer (SEM-EDS JOEL JSM 6510 LA). The magnetic properties were determined using a Vibrating Sample Magnetometer (VSM Oxford Type 1.2 T). UV-Vis Diffuse Reflectance Spectroscopy (UV-Vis DRS Pharmaspec UV-1700) was used to determine

absorption and band gaps. The optical band gap value can be calculated by the equation (Equation 1):

$$(\alpha hv)^n = A\,(hv - Eg) \quad (1)$$

Where; hv is the photon energy, A is the optical constant, h is the Planck constant, and n indicates 2 or ½ for the direct and indirect transitions, respectively.

The absorbance of Congo red was determined using a UV-Vis Spectrophotometer (Type Orion Aquamate 8000). The λ_{max} for measurement of Congo red concentration was obtained at 498 nm. The mineralization was determined using Total Organic Carbon (TOC Teledyne Tekmar).

2.4 Determination of pHpzc

As much as 25 mL of 0.01 M $NaNO_3$ solution was prepared, and its pH was adjusted to range from 2 to 12 by adding 0.1 M HNO_3 or NaOH. Then, 0.1 g of $MgFe_2O_4$ was added to each Erlenmeyer flask and shaken using a shaker at 150 rpm for 48 h (Hariani et al., 2022). The pH of each solution was then determined using a pH meter (HI 2211 Hanna). A graph of ΔpH versus initial pH is used to calculate the pH pzc. The pHpzc measurement was repeated three times.

2.5 Photocatalytic degradation

The photocatalytic degradation process was carried out in a closed reactor at room temperature. The light source used was visible light irradiation (150 w Xenon lamp) at a distance of 30 cm from the sample. The dye was placed in a quartz pipe (50 mL). Congo red dye was used in a volume of 25 mL at a concentration of 50 mg/L. Then, 0.02 g of $MgFe_2O_4$ was added. The variables of photocatalytic degradation studied were pH effects (3-9), concentrations of Congo red (10, 20, 30, 40, and 50 mg/L), and H_2O_2 concentrations (0.5, 1.0, 1.5, 2.0, and 2.5 mM) over a time range of 0-210 min. Photocatalytic degradation was carried out with three repetitions. The degradation efficiency was determined by the formula (Equation 2).

$$\text{Efficiency}\ (\%) = \frac{C_o - C_t}{C_o} \quad (2)$$

Where; C_o and C_t are the initial and final concentrations of Congo red (mg/L).

After the degradation process, the catalyst is separated from the solution using an external magnet. The reusability of $MgFe_2O_4$ was determined by washing it with ethanol and distilled water, drying it in an oven for 60 min at 70ºC, and reusing it for other photocatalytic degradation processes. The reusability process is carried out according to the optimum conditions of photocatalytic degradation obtained. The experiment was repeated five times to determine the degradation efficiency (Ajabshir and Niasari, 2019; Hariani et al., 2022). Figure 1 shows a schematic diagram of a photocatalytic reactor for the degradation of Congo red dye.

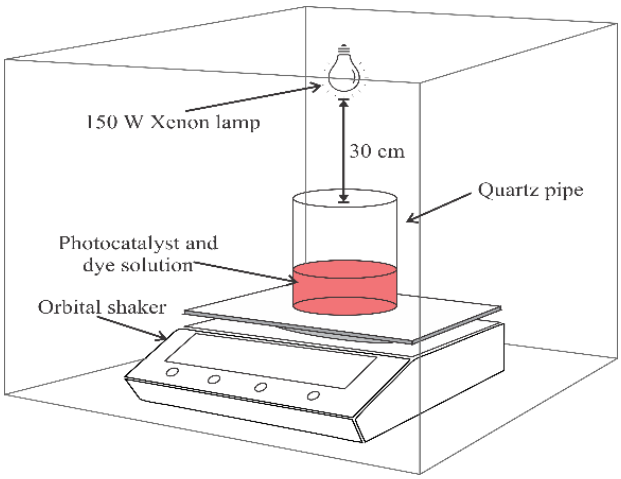

Figure 1. Schematic diagram of a photocatalytic reactor for the degradation of Congo red dye

3. RESULTS AND DISCUSSION

3.1 Characterization of the synthesized $MgFe_2O_4$

The XRD pattern of $MgFe_2O_4$ at 2θ=10-90º is presented in Figure 2. The 2θ angles were observed at 30.19º, 35.55º, 43.13º, 53.95°, 57.70º, 62.64º, and 74.95º, which were of the planes (220), (311), (400), (422), (511), (440), and (553), according to JCPDS card 36-0398, namely cubic spinel structure. The crystallite size of $MgFe_2O_4$ was calculated to be 14.38 nm using the Debye-Scherrer formula on the (311) reflection plane (Shahjuee et al., 2019).

Figure 3(a) shows the absorbance of $MgFe_2O_4$ as determined using UV-DRS. The UV-DRS spectra indicate the wavelength region of the catalyst absorbing light (Fu et al., 2019). It can be seen that the maximum absorption appears at a wavelength of 420 nm which indicates that $MgFe_2O_4$ is more suitable to be used as a catalyst in the visible light region. Based on the extrapolation of the $(\alpha hv)^n$ versus hv curve, the band gap value of $MgFe_2O_4$ was 1.88 eV (Figure 3(b)). The band gap is similar to $MgFe_2O_4$ synthesized using the sol-gel method (1.87 eV) (Vaish et al., 2019) and $MgFe_2O_4$ synthesized using solution combustion (1.91 eV) (Sripiya et al., 2019).

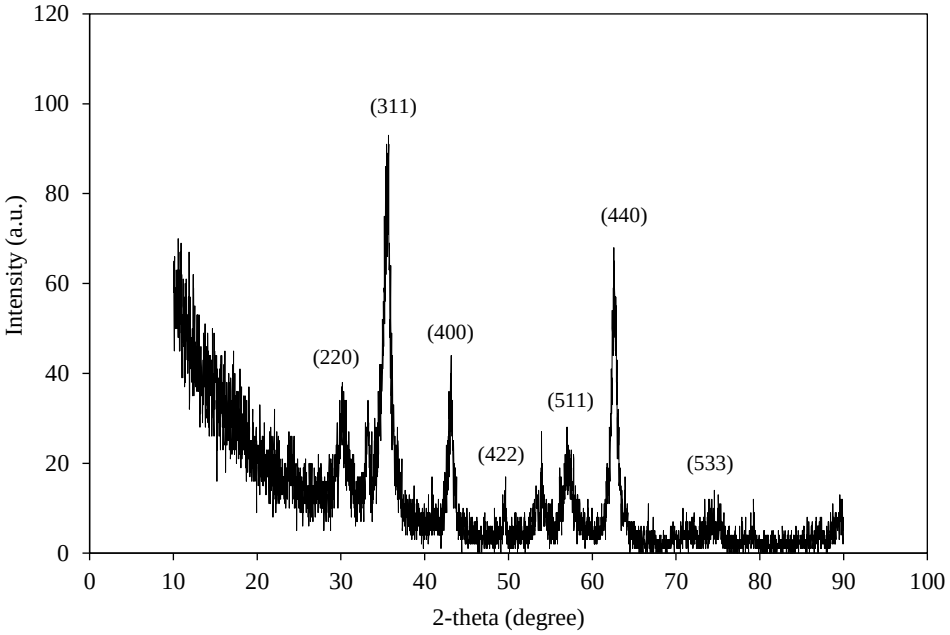

Figure 2. XRD pattern of $MgFe_2O_4$

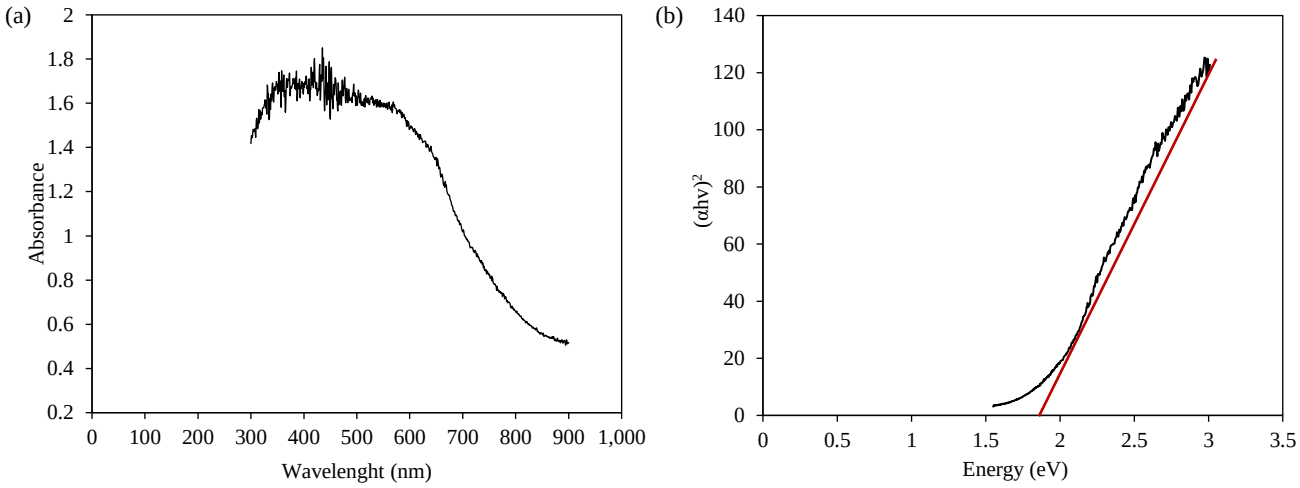

Figure 3. (a) UV-DRS spectrum and (b) band gap of $MgFe_2O_4$

The morphology of $MgFe_2O_4$ is presented in Figure 4. The morphology of $MgFe_2O_4$ appeared to be inhomogeneous; agglomeration occurs in some of it. SEM mapping revealed that Fe (blue) dominated the surface, Mg (red) was almost uniformly distributed, and Oxygen (O) was covered by Fe. The mass percentage of Fe was the highest (59.06%), while O and Mg were 30.26% and 10.68%, respectively. The presence of elements Fe, Mg, and O indicated that the synthesis of $MgFe_2O_4$ was successful.

Figure 5 shows the $MgFe_2O_4$ magnetization curves analysis using VSM. The magnetization curves show superparamagnetic properties. The saturation magnetization value of $MgFe_2O_4$ was 17.78 emu/g, more significant than that of $MgFe_2O_4$ synthesized using tragacanth gum (TG) by the sol-gel method (14 emu/g) (Fardood et al., 2019). $MgFe_2O_4$ is classified as a soft magnetic semiconductor material of the n-type (Maensiri et al., 2009). The saturation magnetization of bulk $MgFe_2O_4$ is approximately 26.9 emu/g (Sepelak et al., 2003). The magnetic property of $MgFe_2O_4$ is an advantage of the catalyst in a photocatalytic degradation process. $MgFe_2O_4$ can be separated from the solution quickly and easily with a permanent magnet after the degradation photocatalytic process.

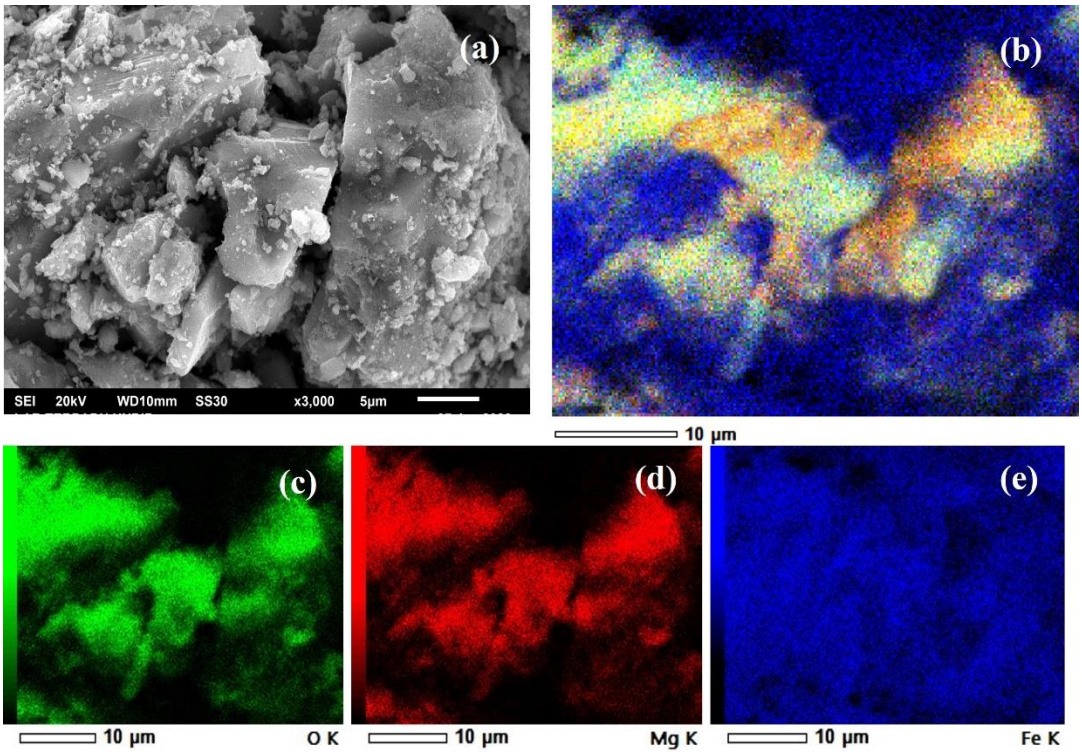

Figure 4. SEM images of (a) $MgFe_2O_4$, (b) elemental mapping of $MgFe_2O_4$, (c) O element, (d) Mg element, and (e) Fe element

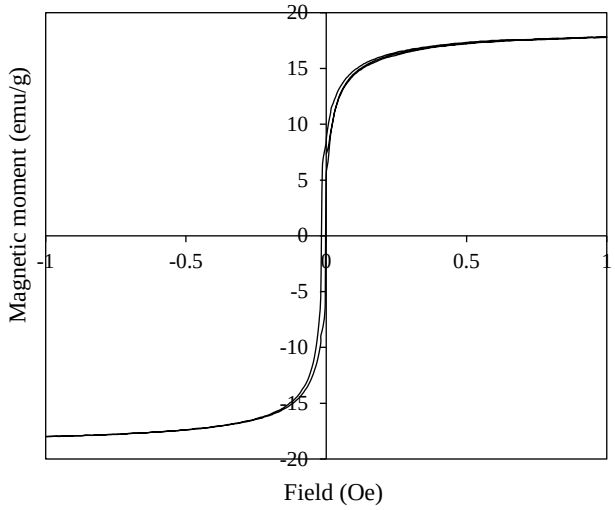

Figure 5. Saturation magnetization curves of $MgFe_2O_4$

3.2 Photocatalytic activity

The pH of the solution affects the interaction between the dye and the catalyst. In a photocatalytic degradation process, the first step is the attraction between the dye and the catalyst. The next step is the decomposition of the dye by two active species, namely superoxide anion ($\bullet O_2^-$) and hydroxyl radical ($\bullet OH$). In a solution with pH > pHpzc, $MgFe_2O_4$ is negatively charged. $MgFe_2O_4$ is positively charged if the pH of the solution < pHpzc. This study found a pHpzc of 6.8 (Figure 6(a)). pH effect was studied using a dye concentration of 50 mg/L in as much as 25 mL with 0.02 g of $MgFe_2O_4$ in the pH range of 3-9 and irradiation time of 0-210 min, as shown in Figure 6(b). The degradation efficiency increases with increasing pH of the solution, with a maximum degradation efficiency of 68.45% at pH 6. The pKa of Congo red dye at room temperature (25°C) is 4.1. Congo red dissociates into a polar group, specifically a negatively charged sulfonate group (R-SO_3-), under acidic conditions (Lafi et al., 2019). At a solution pH < pHpzc, $MgFe_2O_4$ is positively charged, increasing the attraction between the dye and $MgFe_2O_4$ (Shaban et al., 2019). Conversely, there is repulsion between $MgFe_2O_4$ and dyes at an alkaline pH because both are negatively charged (Hariani et al., 2021; Saleh and Taufik, 2019).

The effect of Congo red concentration was observed in the concentration range of 10-50 mg/L in as much as 25 mL with a mass of 0.02 g of $MgFe_2O_4$ and a pH of 6, as shown in Figure 6(c). The highest degradation efficiency occurred at a concentration of 10 mg/L. The elevated dye concentration results in an increased quantity of dye molecules that require decomposition by a restricted quantity of hydroxyl radicals. There is an inverse relationship between dye concentrations and degradation efficiency, whereby higher concentrations of dye lead to lower degradation efficiency (Boudiaf et al., 2021). In addition, the high

dye concentration can block light from interacting with the catalyst, thereby reducing the hydroxyl radicals generated (Vasiljevic et al., 2020; Jha and Chakraborty, 2020). This is similar to other research for the degradation of Congo red using $CoAl_2O_4$/ZnO under visible light irradiation. The photocatalytic degradation reactions are as follows (Jarariya, 2022; Ammar et al., 2020):

$$MgFe_2O_4 + hv \rightarrow MgFe_2O_4 (e_{CB^-} + h_{VB^+}) \quad (3)$$

$$e_{CB^-} + O_2 \rightarrow {}^{\bullet}O_2^- \quad (4)$$

$$h_{VB^+} + H_2O \rightarrow H^+ + {}^{\bullet}OH \quad (5)$$

$${}^{\bullet}O_2^- + H^+ \rightarrow {}^{\bullet}OH_2 \quad (6)$$

$${}^{\bullet}O_2^- + H_2O \rightarrow {}^{\bullet}HO_2 + OH^- \quad (7)$$

$${}^{\bullet}OH_2 + H_2O \rightarrow H_2O_2 + {}^{\bullet}OH \quad (8)$$

$$H_2O_2 \rightarrow 2\ {}^{\bullet}OH \quad (9)$$

$${}^{\bullet}O_2^- + \text{Congo red} \rightarrow CO_2 + H_2O + \text{other products} \quad (10)$$

$${}^{\bullet}OH + \text{Congo red} \rightarrow CO_2 + H_2O + \text{other products} \quad (11)$$

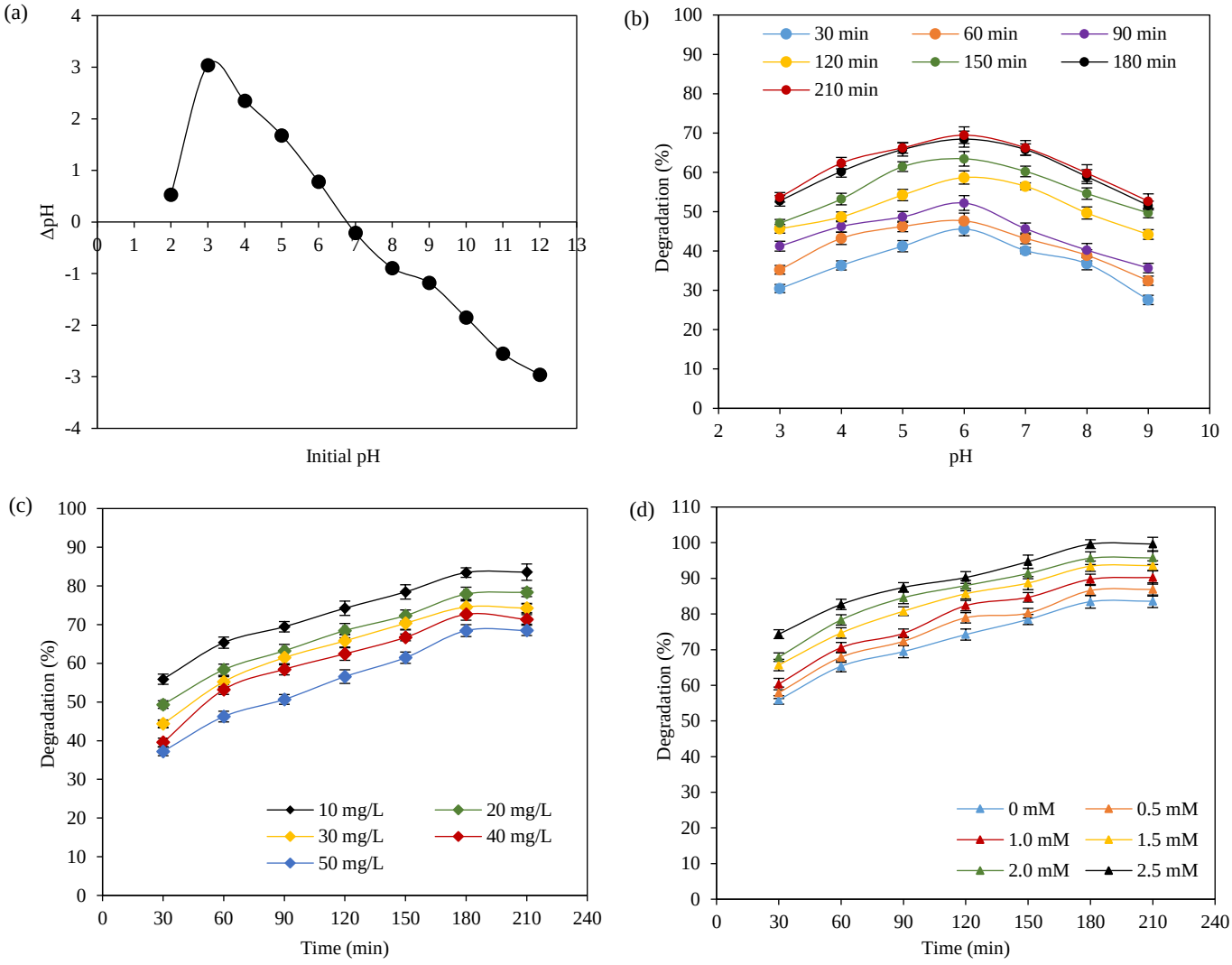

Figure 6. (a) pHpzc of $MgFe_2O_4$ and degradation photocatalytic of Congo red as a function of (b) pH, (c) initial concentration, and (d) H_2O_2 concentration

Figure 6(d) shows the effect of H_2O_2 on the degradation efficiency of Congo red. The dye concentration used was 10 mg/L with a volume of 25 mL, 0.02 g of $MgFe_2O_4$, a solution pH of 6, and H_2O_2 concentrations ranging from 0.5 to 2.5 mM. At 30 to 180 min, it is demonstrated that the greater the H_2O_2 concentration, the more efficient the degradation. No significant difference was observed in the degradation efficiency between the 180 and 210 irradiation times.

The increasing concentration of H_2O_2 also caused the degradation process to become less effective because the ${}^{\bullet}OH$ produced reacted with H_2O_2

reduced the probability of $^{\bullet}OH$ to attack the dye (Saleh and Taufik, 2019). The reactions that occurred were as follows (Flores et al., 2014):

$$^{\bullet}OH + H_2O_2 \rightarrow HO_2^{\bullet} + H_2O \quad (12)$$

$$^{\bullet}OH + HO_2^{\bullet} \rightarrow H_2O_2 + \tfrac{1}{2}O_2 \quad (13)$$

Figure 7 shows the comparison of the degradation efficiency of $MgFe_2O_4$, visible light, H_2O_2, $MgFe_2O_4$ + visible light, and $MgFe_2O_4$ + H_2O_2 + visible light. Sequentially, visible light irradiation (photolysis) < $MgFe_2O_4$ < H_2O_2 < $MgFe_2O_4$ + visible light irradiation < $MgFe_2O_4$ + H_2O_2 + visible light irradiation. The Congo red used had a concentration of 10 mg/L, a volume of 25 mL, 0.02 g $MgFe_2O_4$, a pH of 6, a concentration of H_2O_2 of 2.5 mM, and an irradiation time of 180 min. The results of this study suggest that the $MgFe_2O_4$ and visible light irradiation had the greatest impact on combined effects on degradation efficiency. However, it was also observed that the inclusion of H_2O_2 led to an increase in degradation efficiency. In this study, without the addition of H_2O_2 with an irradiation time of 180 min, the degradation efficiency was 83.45%. Adding H_2O_2 with a concentration of 2.5 mM increased the degradation efficiency to 99.60%. Another study, with an increase in H_2O_2 concentration, revealed that the photocatalytic degradation efficiency of acid orange 7 dye using a ZnO catalyst increased. With the addition of 1.25 mM H_2O_2, its degradation efficiency increased from 38 to 78.9% (Rahmati et al., 2021). Table 1 shows that combined degradation using $MgFe_2O_4$, visible light irradiation and H_2O_2 has the highest degradation efficiency compared to other studies.

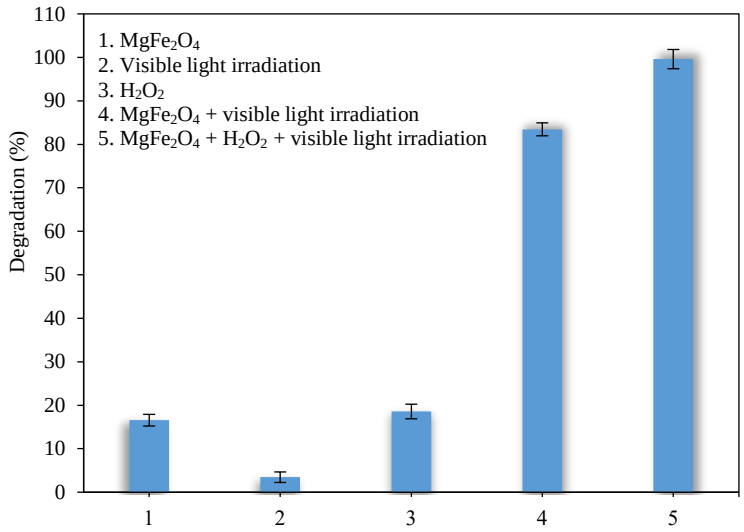

Figure 7. The comparison of the degradation efficiency of $MgFe_2O_4$, visible light irradiation, H_2O_2, $MgFe_2O_4$ + visible light irradiation, and $MgFe_2O_4$ + H_2O_2 + visible light irradiation

Table 1. Comparison of degradation of Congo red using several catalysts

Catalyst	pH	Dose (g/L)	Concentration (mg/L)	Efficiency (%)	References
Cellulose/PVC/ZnO	-	0.6	50	90	Linda et al. (2016)
Bs-$CoFe_2O_4$	9	0.03	5	84	Ali et al. (2020)
Ni-TiO_2	2	0.8	80	92.31	Indira et al. (2021)
$CoAl_2O_4$/ZnO	-	0.1	20	97	Boudiaf et al. (2021)
TiO_2/CoC@SiO_2bipy	4	0.045	10	95.80	Hammud et al. (2022)
SnO_2-Fe_3O_4 + H_2O_2	6	0.03	18	50.76	Said et al. (2022)
$MgFe_2O_4$ + H_2O_2	6	0.02	10	99.62	In this work

3.3 The kinetics of photocatalytic degradation

The kinetics of photocatalytic degradation of Congo red is expressed using the pseudo-first-order kinetics equation as follows (Mahboob et al., 2023; Boudiaf et al., 2021):

$$\ln\left(\frac{C_0}{C}\right) = kt \quad (14)$$

Where; C_o and C is the initial concentration and the concentration after the photocatalytic degradation of Congo red at each time (t), rate constant (k), respectively. Figure 8 shows the kinetics of photocatalytic degradation of Congo red using $MgFe_2O_4$ at a dye concentration of 10 mg/L in as much as 25 mL volume, 0.02 g $MgFe_2O_4$, and pH 6, H_2O_2 2.5 mM under visible light irradiation.

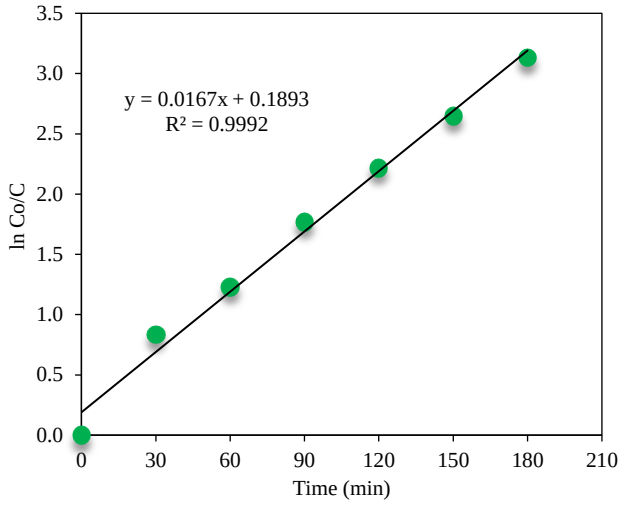

Figure 8. Kinetic photocatalytic degradation of Congo red using $MgFe_2O_4$

The correlation coefficient (R^2) obtained was 0.9992, close to 1, indicating that the photocatalytic degradation was in accordance with the pseudo-first-order. This study determined a k of 0.0167 min^{-1} and a half-life value ($t_{1/2}$=0.693/k) of 41.49 min. Other investigations have demonstrated that the photocatalytic degradation of Congo red employing P-ZrO_2CeO_2ZnO nanoparticles follows a pseudo-first-order with a k of 0.0069 min^{-1} and a $t_{1/2}$ of 100.46 min (Hokonya et al., 2022). Several variables influence the disparity between degradation rates, including catalyst particle size, surface area, work function value (eV), and dye structure (Mandal et al., 2023).

3.4. FTIR spectra before and after photocatalytic degradation

Figure 9 presents the FTIR spectra of $MgFe_2O_4$ before and after being used for Congo red photocatalytic degradation. The broad peak at the wavenumber around 3,400 cm^{-1} represented the O-H vibrations of the adsorbed water molecules. This result was reinforced by the peak at the wavenumber of around 1,630 cm^{-1}, namely H-O-H bending vibrations (Samiei et al., 2018). The characteristics of $MgFe_2O_4$ were observed at wavenumbers in the range 400-800 cm^{-1} attributed to M-O-M stretching (M=Mg and Fe). Wavenumbers around 580 cm^{-1} and 400 cm^{-1} confirm the presence of ferrite structure (Mohdi et al., 2006). The peaks of $MgFe_2O_4$ before and after photocatalytic degradation showed the same characteristics, namely, the wavenumbers appearing at 563 cm^{-1} and 567 cm^{-1} were Fe-O vibrations of tetrahedral and octahedral sites, while those in the area around 422 cm^{-1} and 418 cm^{-1} were the vibrations of octahedral sites. However, some Congo red was adsorbed on $MgFe_2O_4$, as evidenced by the peak at wavenumbers 1,043 cm^{-1} and 1,167 cm^{-1} that was (SO_3) stretching of the sulphonate groups in Congo red dye (Hammud et al., 2022).

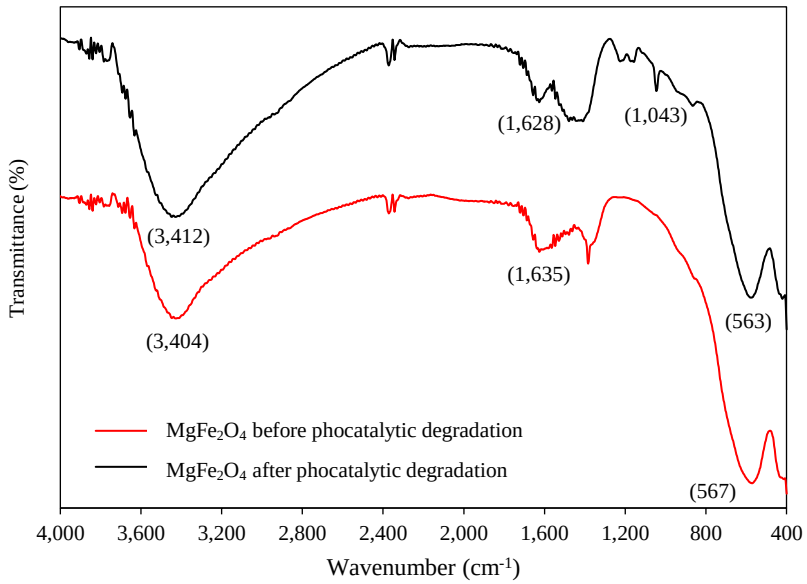

Figure 9. FTIR spectrum of $Mg_2Fe_2O_4$ before and after photocatalytic degradation

3.5. Reusability of the photocatalyst

Determining a catalyst's performance requires testing its regeneration and reuse. $MgFe_2O_4$, after use in the photocatalytic degradation process, was washed and dried in an oven to be reused for photocatalytic degradation at the optimum conditions obtained, namely, Congo red at a concentration of 10 mg/L in a volume of 25 mL, 0.02 g $MgFe_2O_4$, a pH of 6, 2.5 mM H_2O_2, and an irradiation time of 180 min. Figure 10 presents the effectiveness of degradation after five cycles. After five cycles, the effectiveness of photocatalytic degradation decreased from 99.62% to 94.50% (<5%). Such a reduction in the degradation effectiveness can occur during the photocatalytic degradation processes, such as separation, washing, drying processes, and the catalyst can undergo agglomeration (Hariani et al., 2022).

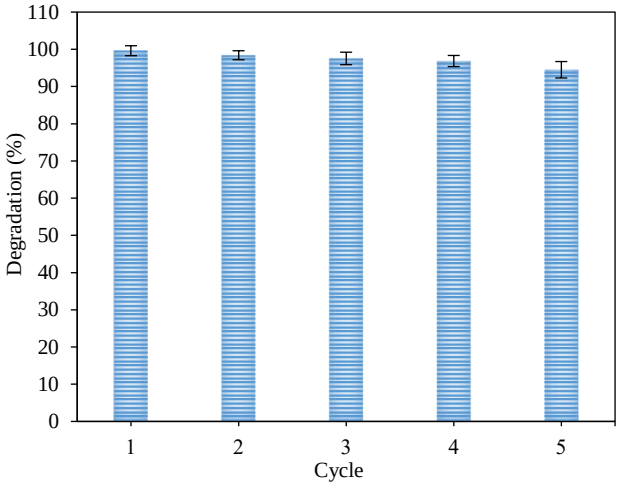

Figure 10. Reusability of $MgFe_2O_4$ as photocatalyst

The level of mineralization of Congo red as a result of photocatalytic degradation is determined from the total organic carbon (TOC) value. Mineralization levels are usually not fully developed (Pourzad et al., 2020). In this study, the TOC values were determined before and after photocatalytic degradation with a dye concentration of 10 mg/L, pH 6, H_2O_2 concentration of 2.5 mM, and irradiation time of 180 min. The TOC removal obtained was 84.58%. Other research indicated that the longer the irradiation time, the higher the effectiveness of TOC. Congo red photocatalytic degradation using $CoAl_2O_4$/ZnO under visible light irradiation obtained a maximum TOC of 66.9% (Boudiaf et al., 2021). A reduction in the TOC value proves that dye mineralization has occurred.

4. CONCLUSION

$MgFe_2O_4$ has been successfully synthesized by the coprecipitation method. The results show that $MgFe_2O_4$ has magnetic properties and, after being used as a photocatalyst, is easily separated from the solution using a permanent magnet. The efficiency of photocatalytic degradation is affected by the pH of the solution, the concentration of dye, and the addition of H_2O_2. The optimum photocatalytic degradation was obtained at a solution pH of 6, a dye concentration of 10 mg/L, a concentration of 2.5 mM H_2O_2, and irradiation time of 180 min under visible light irradiation, with a degradation efficiency of 99.62%. $MgFe_2O_4$ has high stability and reusability because, after five cycles, the degradation efficiency is above 90%. The study indicated that $MgFe_2O_4$ has the potential to be used for wastewater treatment, especially for treating wastewater containing dyes.

ACKNOWLEDGEMENTS

This research was funded by the DIPA of Public Service Agency of Universitas Sriwijaya 2022, SP DIPA-023.17.2.677515/2022 (SATEKS scheme), on December 13th, 2021, in accordance with the Rector's Decree Number: 0110/UN9.3.1/SK/2022, on April 28th, 2022.

REFERENCES

Ajabshir SZ, Niasari MS. Preparation of magnetically retrievable $CoFe_2O_4$-SiO_2-$Dy_2Ce_2O_7$ nanocomposites as novel photocatalyst for higly efficient degradation of organic contaminants. Composites Part B: Engineering 2019;174:1-9.

Ali N, Said A, Ali F, Razig F, Ali Z, Bilil M, et al. Photocatalytic degradation of Congo red dye from aqueous environment using cobalt ferrite nanostructures: Development, characterization, and photocatalytic performance. Water, Air, and Soil Pollution 2020;231(50):1-16.

Ammar SH, Elaibi AI, Mohamme IS. Core/shell Fe_3O_4@Al_2O_3-PMo magnetic nanocatalyst for photocatalytic degradation of organic pollutants in an internal loop airlift reactor. Journal of Water Process Engineering 2020;37:Article No.101240.

Argote-Fuentes S, Feria-Reyes R, Ramos-Ramirez E, Gutierrez-Ortega N, Cruz-Jimenez G. Photoelectrocatalytic degradation of Congo red dye with activated hydrotalcites and copper anod. Catalysts 2021;11(211):1-19.

Augugliaro V, Bellardita M, Loddo V, Palmisano G, Palmisano L, Yurdakal S. Overview on oxidation mechanisms of organic compounds by TiO_2 in heterogeneous photocatalysis. Journal of Photochemistry and Photobiology C: Photochemistry Reviews 2012;3(3):224-45.

Boudiaf S, Nasrallah N, Mellal M, Belhamdi B, Belabed C, Djilali MA, et al. Kinetic studies of congo red photodegradation on the hetero-system $CoAl_2O_4$/ZnO with a stirred reactor under solar light. Journal of Environmental Chemical Engineering 2021;9(4):Article No.105572.

El Gaini L, Lakraimi M, Sebbar E, Meghea A, Bakasse M. Removal of indigo carmine dye from water to Mg-Al-CO_3-calcined layered double hydroxides. Journal of Hazardous Materials 2009;161(2-3):627-32.

Fardood ST, Moradnia F, Mostafaei M, Afshari Z, Faramarzi V. Biosynthesis of $MgFe_2O_4$ magnetic nanoparticles and their application in photodegradation of malachite green dye and kinetic study. Nanochemistry Research 2019;4(1):86-93.

Flores A, Nesprias K, Vitale P, Tasca J, Lavat A, Eyler N, et al. Heterogeneous photocatalytic discoloration/degradation of rhodamine B with H_2O_2 and spinel copper ferrite magnetic nanoparticles. Australian Journal of Chemistry 2014;67:609-14.

Fu C, Liu X, Wang Y, Li L, Zhang Z. Preparation and characterization of Fe_3O_4@SiO_2@TiO_2-Co/rGO magnetic visible light photocatalyst for water treatment. RSC Advances 2019;9:20256-65.

Gao HJ, Wang SF, Fang LM, Sun GA, Chen XP, Tang SN, et al. Nanostructured spinel-type M (M=Mg, Co, Zn) Cr_2O_4 oxides: Novel adsorbents for aqueous Congo red removal. Materials Today Chemistry 2021;22:Article No.100593.

Habiba U, Siddique TA, Joo TC, Salleh A, Ang BC, Afifi AM. Synthesis of chitosan/polyvinyl alcohol/zeolite composite for removal of methyl orange, Congo red and chromium(VI) by flocculation/adsorption. Carbohydrate Polymers 2017;157: 1568-76.

Hammud HH, Traboulsi H, Karnati RK, Bakir EM. Photodegradation of Congo red by modified P25-titanium dioxide with cobalt-carbon supported on SiO_2 matrix, DFT studies of chemical reactivity. Catalyst 2022;12(248):1-14.

Hariani PL, Said M, Rachmat A, Riyanti F, Pratiwi HC, Rizki WT. Preparation of $NiFe_2O_4$ nanoparticles by solution combustion method as photocatalyst of Congo red. Bulletin of Chemical Reaction Engineering and Catalysis 2021;16:481-90.

Hariani PL, Said M, Salni, Aprianti N, Naibaho YALR. High efficient photocatalytic degradation of methyl orange dye in an aqueous solution by $CoFe_2O_4$-SiO_2-TiO_2 magnetic catalyst. Journal of Ecological Engineering 2022;23:118-28.

Harja M, Buema G, Bucur D. Recent advances in removal of Congo red dye by adsorption using an industrial waste. Scientific Reports 2022;12(6087):1-18.

Hokonya N, Mahamadi C, Mukaratirwa-Muchanyereyi N, Gutu T, Zvinowanda C. Green synthesis of P-ZrO_2CeO_2ZnO nanoparticles using leaf extracts of *Flacourtia indica* and their application for the photocatalytic degradation of a model toxic dye, Congo red. Heliyon 2022;8:1-18.

Indira K, Shanmugam S, Hari A, Vasantharaj S, Sathiyavimal S, Brindhadevi K, et al. Photocatalytic degradation of Congo red dye using nickel-titanium dioxide nanoflakes synthesized by *Mukia madrasapatna* leaf extract. Environmental Research 2021;202:1-8.

Jarariya R. A review based on spinel ferrite nanomaterials-$MgFe_2O_4$-synthesis of photocatalytic dye degradation in visible light response. Journal of Environmental Treatment Techniques 2022;10(2):149-56.

Jha AK, Chakraborty S. Photocatalytic degradation of Congo red under UV irradiation by zero valent iron nano particles (nZVI) synthesized using *Shorea robusta* (Sal) leaf extract. Water Science and Technology 2020;82(11):2491-502.

Khumalo NP, Nthunya LN, De Canck E, Derese S, Verliefde AR, Kuvarega AT, et al. Congo red dye removal by direct membrane distillation using PVDF/PTFE membrane. Separation and Purification Technology 2019;211:578-86.

Lafi R, Montasser I, Hafiane A. Adsorption of Congo red dye from aqueous solutions by prepared activated carbon with oxygen-containing functional groups and its regeneration. Adsorption Science and Technology 2019;37(1-2):160-81.

Linda T, Muthupoongodi S, Shajan XS, Balakumur S. Photocatalytic degradation of Congo red and crystal violet dyes on cellulose/PVC/ZnO composites under UV light irradiation. Materials Today: Proceedings 2016;3:2035-41.

Lum PT, Foo KY, Zakaria NA, Palaniandy P. Ash based nanocomposites for photocatalytic degradation of textile dye pollutants: A review. Materials Chemistry and Physics 2020;241:Article No.122405.

Maensiri S, Sangmanee M, Wiengmoon A. Magnesium Ferrite ($MgFe_2O_4$) nanostructures fabricated by electrospinning. Nanoscale Research Letter 2009;4:221-8

Mandal RK, Mondal AS, Ghosh S, Halder A, Majumder TP. Synthesis, characterisation and optical studies of CdO-NiO NCs for comparative dye degradation study between two hazardous dyes Congo red and rose bengal. Results in Chemistry 2023;5:Article No.100810.

Mahboob I, Shafig I, Shafique S, Akhter P, Munir M, Saeed M, et al. Porous Ag_3VO_4/KIT-6 composite: Synthesis, characterization and enhanced photocatalytic performance for degradation of Congo red. Chemosphere 2023;311:Article No.137180.

McDonald KD, Bartlett BM. Microwave synthesis of spinel $MgFe_2O_4$ nanoparticles and the effect of annealing on photocatalysis. Inorganic Chemistry 2021;60:8704-9.

Mezohegyi G, Van Der Zee FP, Font J, Fortuny A, Fabregat A. Towards advanced aqueous dye removal processes: A short review on the versatile role of activated carbon. Journal of Environmental Management 2012;102:148-64.

Mohdi KB, Chhantbar MC, Joshi HH. Study of elastic behavior of magnesium ferri aluminates. Ceramics International 2006; 32(2):111-4.

Nguyen LTT, Nguyen LTH, Manh NC, Quoc DN, Quang HN, Nguyen HTT, et al. A facile synthesis, characterization, and photocatalytic activity of magnesium ferrite nanoparticles via the solution combustion method. Journal of Chemistry 2019;2019:Article No.3428681.

Oliveira TP, Marques GN, Castro MAM, Costa RCV, Rangel JHG, Rodrigues SF, et al. Synthesis and photocatalytic investigation of $ZnFe_2O_4$ in the degradation of organic dyes under visible light. Journal of Materials Research and Technology 2020;9(6):15001-15.

Pourzad A, Sobhi HR, Behbahani M, Esrafili A, Kalantary RR, Kermani M. Efficient visible light-induced photocatalytic removal of paraquat using N-doped TiO_2@SiO_2@Fe_3O_4 nanocomposite. Journal of Molecular Liquids 2020;299: Article No.112167.

Rahmati R, Nayebi B, Ayati B. Investigating the effect of hydrogen peroxide as an electron acceptor in increasing the capability of slurry photocatalytic process in dye removal. Water Science and Technology 2021;83(10):2414-23.

Robinson T, McMullan G, Marchant R, Nigam P. Remediation of dyes in textile effluent: A critical review on current treatment technologies with a proposed alternative. Bioresource Technology 2001;77(3):247-55.

Saha R, Mukhopadhyay M. Elucidation of the decolorization of Congo red by trametes versicolor laccase in presence of ABTS through cyclic voltammetry. Enzyme and Microbial Technology 2020;135:Article No.109507.

Said M, Rizki WT, Asri WR, Desnelli D, Rachmat A, Hariani PL. SnO_2-Fe_3O_4 nanocomposites for the photodegradation of the Congo red dye. Heliyon 2022;8:1-8.

Saleh R, Taufik A. Degradation of methylene blue and Congo red dyes using Fenton, photo-Fenton, sono-Fenton, and sonophoto-Fenton methods in the presence of iron (II,III) oxide/zinc oxide/graphene (Fe_3O_4/ZnO/graphene) composites. Separation and Purification Technology 2019;210:563-73.

Samiei S, Pakpur F, Ghanbari D. Synthesis of magnesium ferrite-silver nanostructures and investigation of its photocatalyst and magnetic properties. Journal of Nanostructures 2018; 8(1):37-46.

Sathiskumar K, Alsalhi MS, Sanganyado E, Devanesan S, Arulprakash A, Rajasekar A. Sequential electrochemical oxidation and bio-treatment of the azo dye Congo red and textile effluent. Journal of Photochemistry and Photobiology B: Biology 2019;200:Article No.111655.

Sepelak V, Baabe D, Mienert D, Litterst FJ, Becker KD. Enhanced magnetisation in nanocrystalline high-energy milled $MgFe_2O_4$. Scripta Materialia 2003;48:961-6.

Shaban M, Ahmed AM, Shehata N, Betiha MA, Rabie AM. Ni-doped and Ni/Cr co-doped TiO_2 nanotubes for enhancement of photocatalytic degradation of methylene blue. Journal of Colloid and Interface Science 2019;555:31-41.

Shahid M. Jingling L, Ali Z, Shakir I, Warsi MF, Parveen R, et al. Photocatalytic degradation of methylene blue on magnetically separable $MgFe_2O_4$ under visible light irradiation. Materials Chemistry and Physics 2013;139:566-71.

Shahjuee T, Masoudpanah SM, Mirkazemi SM. Thermal decomposition synthesis of $MgFe_2O_4$ nanoparticles for magnetic hyperthermia. Journal of Superconductivity and Novel Magnetism 2019;32:1347-52.

Sharma G, Algarni TS, Kumar PS, Bhogal S, Kumar A, Sharma S, et al. Utilization of Ag_2O-Al_2O_3-ZrO_2 decorated onto rGO as adsorbent for the removal of Congo red from aqueous solution. Environmental Research 2021;197:Article No.111179.

Sripiya R, Mahendiran M, Madahavan J, Raj MVA. Enhanced magnetic properties of $MgFe_2O_4$ nanoparticles. Materials Today: Proceedings 2019;8:310-4.

Vaish G, Kripal R, Kumar L. EPR and optical studies of pure $MgFe_2O_4$ and ZnO nanoparticles and $MgFe_2O_4$-ZnO nanocomposite. Journal of Materials Science: Materials in Electronics 2019;30:16518-26.

Valenzuela MA, Bosch P, Jimenez-Becerrill J, Quiroz O, Paez AI. Preparation, characterization and photocatalytic activity of ZnO, Fe_2O_3 and $ZnFe_2O_4$. Journal of Photochemistry and Photobiology A: Chemistry 2002;148(1-3):177-82.

Vasiljevic ZZ, Dojcinovic MP, Vujancevic JD, Jankovic-Casvan I, Ognjanovic M, Tadic NB, et al. Photocatalytic degradation of methylene blue under natural sunlight using iron titanate nanoparticles prepared by a modified sol-gel method. Royal Society Open Science 2020;7:1-14.

Wang L, Li J, Wang Y, Zhao L, Jiang Q. Adsorption capability for Congo red on nanocrystalline MFe_2O_4 (M=Mn, Fe, Co, Ni) spinel ferrites. Chemical Engineering Journal 2012;181-182:72-9.

Zhang J, Fan S, Lu B, Cai Q, Zhao J, Zang S. Photodegradation of naphthalene over Fe_3O_4 under visible light irradiation. Royal Society Open Science 2019;6:1-15.